# Active Forces in Confluent Cell Monolayers

Guanming Zhang* and Julia M. Yeomans
*Department of Physics, The Rudolf Peierls Centre for Theoretical Physics, University of Oxford, Parks Road, Oxford OX1 3PU, United Kingdom*

(Received 13 December 2021; accepted 22 December 2022; published 20 January 2023)

We use a computational phase-field model together with analytical analysis to study how intercellular active forces can mediate individual cell morphology and collective motion in a confluent cell monolayer. We explore the regime where intercellular forces dominate the tissue dynamics, and polar forces are negligible. Contractile intercellular interactions lead to cell elongation, nematic ordering, and active turbulence characterized by motile topological defects. Extensile interactions result in frustration, and perpendicular cell orientations become more prevalent. Furthermore, we show that contractile behavior can change to extensile behavior if anisotropic fluctuations in cell shape are considered.

DOI: 10.1103/PhysRevLett.130.038202

*Introduction.*—Asking how cells move collectively is a fascinating and important problem that encompasses both the concepts of forces and flows traditional to physics [1,2] and the molecular signaling which drives many biological phenomena [3]. Generic descriptions of cell motility, such as the phase-field model [4–11] and vertex models [12–16], have recently contributed to understanding several aspects of cell motility.

The forces driving single cells across a flat surface are well understood. The cell is controlled by directional actin filaments, which can continuously polymerize and depolymerize to produce lamellopodia, protrusions that push the cell forward [17,18]. To advance, the cell needs to push against the substrate, and to do this effectively it creates focal adhesions, which are mechanical links between internal actin bundles and the external surface [19]. As it moves, the cell tends to polarize and elongate in the direction of motion [20]. Contractile forces mediated by myosin motors interacting with the actin network within the cell tend to restore it to circular [21]. Thus, a minimal physical model of single cell motility comprises a net force in the direction of the cell polarity, together with contractile, balanced forces restoring the cell to a circular shape. [We will refer to forces that tend to return an elongated cell to circular, or to extend it further, as contractile and extensile, respectively; Fig. 1(a)].

Much less is understood about the dynamics of confluent cell layers. The cells can be jammed with local fluctuations [13,22] or form liquidlike states where the motion has localized, correlated bursts of velocity or vorticity. Moreover, motile topological defects, regions where the long axes of the cells take comet or trefoil-like configurations [Figs. 1(b) and 1(c)], have been identified in several confluent cell layers [23–26]. This is reminiscent of active turbulence, which is the dynamical behavior of many active nematic materials, such as suspensions of microswimmers [27,28] or microtubules driven by motor proteins [27]. However, the appearance of active turbulence requires elongated particles [29], and therefore, it is somewhat surprising to identify topological defects even in assemblies of, e.g., Madin-Darby canine kidney cells that are on average isotropic in shape [25]. Moreover, the comet defects can move toward their head, corresponding to extensile driving [30], even though individual cells are contractile [24]. Indeed, experiments and simulations have shown that the defect motion changes direction—indicating a change from extensile to contractile behavior—as the cell-cell adhesion is varied. Other theoretical work has

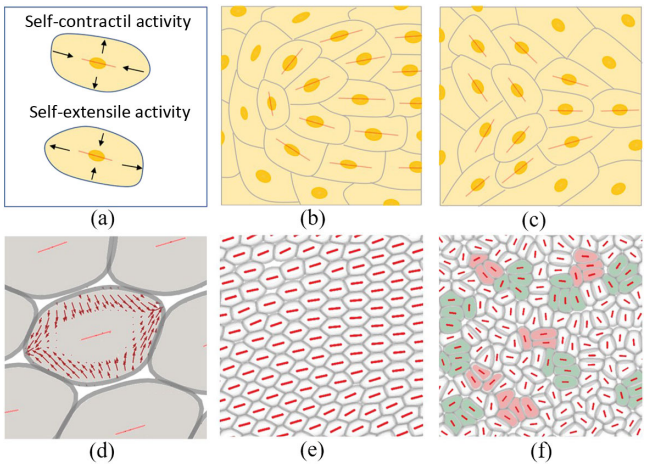


FIG. 1. (a) Self-deformation activity. (b) Schematic of $+1/2$ defect. (c) Schematic of $-1/2$ defect. (d) Intercellular contractile forces act on the central cell as a self-extensile force. (e) Nematic ordering in tissue with contractile intercellular forces [$\omega = 0.5$, $\zeta_{\text{inter}} = -0.6$ for (d) and (e)]. (f) "Capped line" structures (distinguished as red and green regions) in tissue with extensile intercellular forces. Red bars indicate cell elongation axes.

 

shown that fluctuating polar (unbalanced) forces can result in extensile or contractile defects [31–33].

These observations raise questions about the identity of the physical forces governing collective cell motility. It has been argued that the formation of lamellopodia is suppressed in confluent cell layers, a phenomenon termed contact inhibition of locomotion, suggesting a reduction in the strength of any persistent, unbalanced (polar) force [34,35], although it is not yet clear whether fluctuating polar forces are also suppressed [1]. Here we assume that we can ignore any polar contributions in which case balanced forces must be acting to drive the cellular dynamics and, because the cells continue moving, these must be active, i.e., continuously fueled by chemical energy. The most likely physical origin for these are the forces between cells which act through adherens junctions between a cell and its neighbors [2]. Therefore, we present analytical arguments and simulations based on a two-dimensional, coarse-grained, phase-field model of cell motility to show that active, contractile interactions between cells, mediated through cell junctions, lead to the cells elongating and lining up to give nematic ordering. Decreasing cell-cell adhesion leads to flows which destabilize the nematic order, resulting in active turbulence and contractile topological defects. We further show that anisotropic fluctuations of the intercellular forces can change the direction in which the defects move.

*Model.*—The phase-field approach describing the dynamics of a confluent cell layer resolves individual cells and their interactions but not the internal cell machinery [4,7,36,37]. Each cell $i$ is represented by an individual phase field, $\varphi^{(i)}(\mathbf{x})$. The motion of each phase field is governed by a local velocity field $\mathbf{v}^{(i)}(\mathbf{x})$ according to the equation of motion

$$\partial_t \varphi^{(i)}(\mathbf{x}) + \mathbf{v}^{(i)}(\mathbf{x}) \cdot \nabla \varphi^{(i)}(\mathbf{x}) = -J_0 \frac{\delta \mathcal{F}}{\delta \varphi^{(i)}(\mathbf{x})}, \quad (1)$$

where $\mathcal{F}$ is a free energy. $-J_0[(\delta\mathcal{F})/(\delta\varphi^{(i)})]$ describes the relaxation dynamics of the cells to a free-energy minimum at a rate $J_0$. Assuming overdamped dynamics, the velocity $\mathbf{v}^{(i)}(\mathbf{x})$ of a cell is determined by the local force density acting on the cell,

$$\xi \mathbf{v}^{(i)}(\mathbf{x}) = \mathbf{f}^{(i)}_{\text{passive}}(\mathbf{x}) + \mathbf{f}^{(i)}_{\text{active}}(\mathbf{x}), \quad (2)$$

where $\xi$ is a friction coefficient.

The passive force density $\mathbf{f}^{(i)}_{\text{passive}}(\mathbf{x}) = [(\delta\mathcal{F})/(\delta\varphi^{(i)})]\nabla\varphi^{(i)}$ includes a Cahn-Hilliard term that encourages $\varphi^{(i)}$ to take values 1, which we choose to correspond to the inside of the cell $i$, or 0, which denotes the region outside the cell, a soft constraint, restricting the area of each cell, a repulsion energy that penalizes overlap between cells and, of particular relevance here, a cell-cell adhesion energy with strength parametrized by $\omega$. See Supplemental Material [38] and Refs. [4,6,8,40] for more details.

To formulate the active contribution to the force density $\mathbf{f}^{(i)}_{\text{active}}(\mathbf{x})$, we first calculate the deformation tensor that quantifies the shape of a cell [4,41],

$$\begin{aligned}\mathcal{D}^{(i)} &= -\int d\mathbf{x}\left\{\nabla\varphi^{(i)}\nabla\varphi^{(i)^T} - \frac{\mathbb{1}}{2}\mathrm{Tr}(\nabla\varphi^{(i)}\nabla\varphi^{(i)^T})\right\} \\ &\equiv \sqrt{(\mathcal{D}^{(i)}_{xx})^2 + (\mathcal{D}^{(i)}_{xy})^2}\left(\mathbf{d}^{(i)}_{\parallel}\mathbf{d}^{(i)^T}_{\parallel} - \mathbf{d}^{(i)}_{\perp}\mathbf{d}^{(i)^T}_{\perp}\right), \end{aligned} \quad (3)$$

where $\mathbf{d}^{(i)}_{\parallel}$ and $\mathbf{d}^{(i)}_{\perp}$ are the orthonormal eigenvectors of the $\mathcal{D}^{(i)}$, along and perpendicular to the elongation axis of the cell, respectively, normalized so that $\mathbf{d}^{(i)}_{\parallel}\mathbf{d}^{(i)^T}_{\parallel} + \mathbf{d}^{(i)}_{\perp}\mathbf{d}^{(i)^T}_{\perp} = \mathbb{1}$.

We next define a director $\boldsymbol{n}^{(i)}$ associated with each cell $i$ and assume that $\boldsymbol{n}^{(i)}$ relaxes toward $\mathbf{d}^{(i)}_{\parallel}$ through a stochastic relaxation process,

$$\frac{d\mathbf{n}^{(i)}}{dt} = J_n\left(\mathbf{d}^{(i)}_{\parallel} - \mathbf{n}^{(i)}\right) + \boldsymbol{\eta}^{(i)}(t). \quad (4)$$

$J_n$ controls the timescale of relaxation. We assume anisotropic, Gaussian noise uncorrelated between cells, with

$$\begin{aligned}\langle\boldsymbol{\eta}(t)\rangle &= \mathbf{0}, \\ \langle\boldsymbol{\eta}^{(i)}(t)\boldsymbol{\eta}^{(i)}(t')^T\rangle &= \delta(t-t')\left(D_{\parallel}\mathbf{d}^{(i)}_{\parallel}\mathbf{d}^{(i)^T}_{\parallel} + D_{\perp}\mathbf{d}^{(i)}_{\perp}\mathbf{d}^{(i)^T}_{\perp}\right). \end{aligned} \quad (5)$$

The variance of the noise couples to the shape of the cell and can take different values for fluctuations along $\mathbf{d}^{(i)}_{\parallel}$ or $\mathbf{d}^{(i)}_{\perp}$.

In the absence of any unbalanced active forces, the leading order contribution to the active stress acting on cell $i$ is related to the director field by [42]

$$\sigma^{(i)}_{\alpha\beta}(\mathbf{x}) = -\zeta_{\text{self}} Q^{(i)}_{\alpha\beta}\varphi^{(i)}(\mathbf{x}) - \zeta_{\text{inter}}\sum_{j\neq i} Q^{(j)}_{\alpha\beta}\varphi^{(j)}(\mathbf{x}), \quad (6)$$

where

$$Q^{(i)}_{\alpha\beta} = \left\{(n^{(i)}_{\alpha}n^{(i)}_{\beta} - \frac{|\boldsymbol{n}^{(i)}|^2}{2}\delta_{\alpha\beta}\right\}. \quad (7)$$

We distinguish between the stress acting on cell $i$ due to internal forces, of strength $\zeta_{\text{self}}$, and that due to other cells, of strength $\zeta_{\text{inter}}$. $\zeta_{\text{self}}$ and $\zeta_{\text{inter}}$ are not necessarily the same. They both rely on actomyosin contractility, but the former is mediated by linker proteins such as ezrin, radixin and moesin proteins connecting a cell's actomyosin networks to its membrane [43,44], whereas the latter relies upon force transmission between cells mediated by cadherin-based

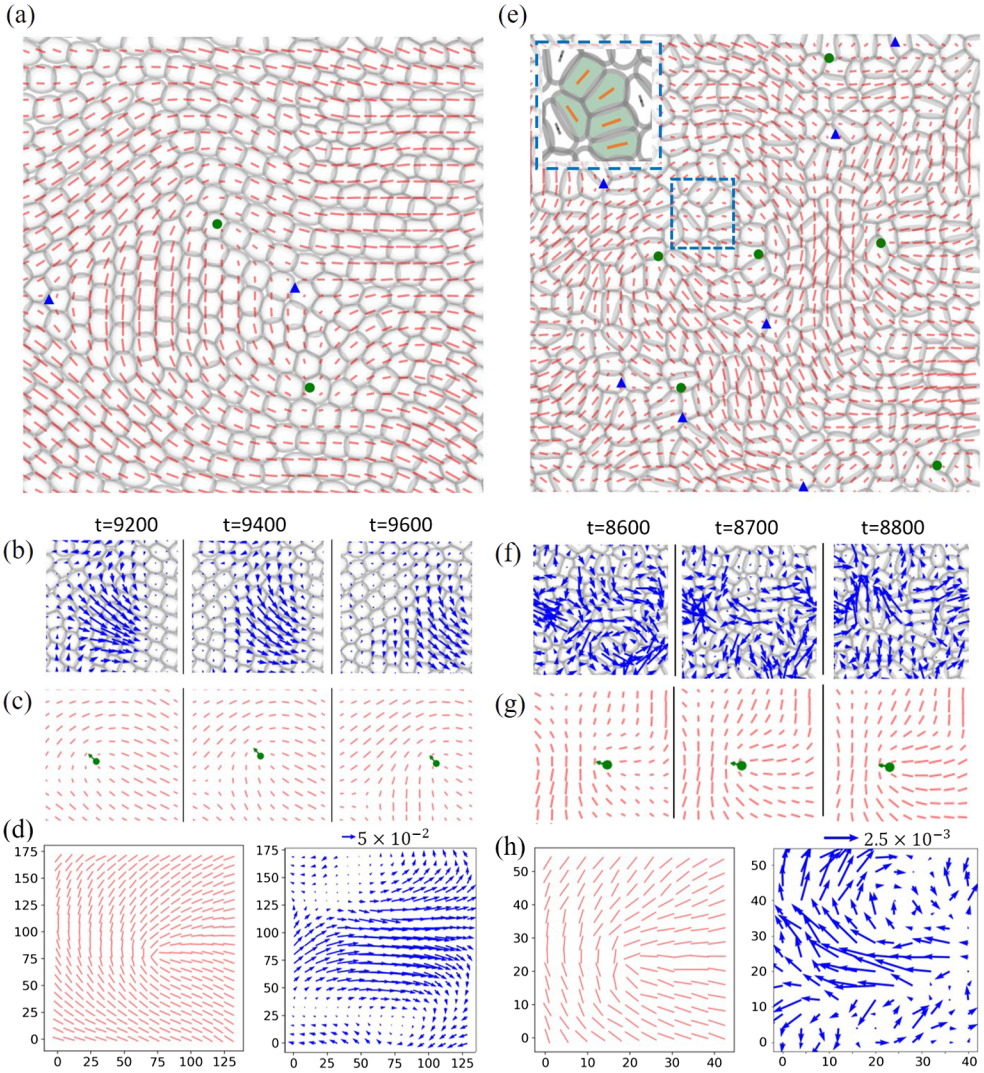


FIG. 2. Cell and defect dynamics driven by intercellular forces. Left column: contractile intercellular forces $\zeta_{\text{inter}} = -0.6$, $\omega = 0$. Right column: extensile intercellular forces $\zeta_{\text{inter}} = +0.4$, $\omega = 0$. (a),(e) Simulation snapshots. Red lines indicate the coarse-grained field of elongation axes. Green dots and blue triangles indicate $+1/2$ cometlike and $-1/2$ trefoil-like defects. The subframe of (e) shows the capped line cell configuration. (b) and (f) Cell configuration around a $+1/2$ defect with imposed velocity field (blue arrows) at successive times. (c) and (g) Corresponding images showing the elongation axes field and the defect motion. The defect moves toward its tail (head) in the contractile (extensile) system. (d) and (h) Averaged cell elongation axes (left) and velocity (right) fields in the vicinity of a defect [86 and 325 $+1/2$ defects are averaged for (d) and (h), respectively]. Note the scale change between the contractile and extensile cases. Similar results for $-1/2$ defects are given in Fig. S2 of the Supplemental Material [38].

junctions [2]. Our arguments are not changed qualitatively by a self-contractility that is small compared to the intercellular term, and therefore, we choose $\zeta_{\text{self}} = 0$ to study the effect of the intercellular forces alone [compare Fig. S1 in the Supplemental Material [38] and Figs. 2(a) and 2(e)].

The force density arising from the active stress is then

$$\mathbf{f}^{(i)}_{\text{active}}(\mathbf{x}) = \nabla \cdot \boldsymbol{\sigma}^{(i)} = -\zeta_{\text{inter}} \sum_{j \neq i} \mathbf{Q}^{(j)} \cdot \nabla \varphi^{(j)}(\mathbf{x}). \quad (8)$$

*Intercellular contractile forces.*—Individual cells are contractile, so a plausible physical picture is that a cell feels the contractile forces from its neighbors, transmitted through cell-cell junctions. Therefore, we first investigate contractile, intercellular forces ($\zeta_{\text{inter}} < 0$), assuming instantaneous relaxation of the director to the elongation axis of the cell ($\mathbf{n}^{(i)} = \mathbf{d}^{(i)}_{\parallel}$). Figure 1(d) shows the typical force density acting on a given cell due to its contractile neighbors. Surprisingly, the cell is stretched.

This can be explained by considering Eq. (8). The gradient of a phase-field $\nabla \varphi^{(i)}$ points perpendicular to a cell boundary toward the cell center. In addition, in a confluent monolayer with strong cell-cell adhesion, cells nestle closely sharing common interfaces. These properties allow us to approximate $\nabla \varphi^{(j)} \approx -\nabla \varphi^{(i)}$ at cell-cell overlap

(measured by $\varphi^{(i)}\varphi^{(j)}$) for the dominant contributions in Eq. (8), so the active intercellular force can be written

$$\mathbf{f}^{(i)}_{\text{active}}(\mathbf{x}) \approx +\zeta_{\text{inter}}\mathbf{Q}^{(i)}_{\text{eff}} \cdot \nabla\varphi^{(i)}(\mathbf{x}) \tag{9}$$

in terms of an effective $\mathbf{Q}$-tensor field $\mathbf{Q}^{(i)}_{\text{eff}} = \varphi^{(i)} \sum_{j\neq i} \mathbf{Q}^{(j)}\varphi^{(j)}$. The change in sign shows that a cell with contractile neighbors will be subject to an extensile-like, self-deformation force density [Fig. 1(a)] which stretches the cell [Fig. 1(d)]. Moreover, Eq. (9) shows that each cell tends to align along the average elongation direction of its neighbors which, following the usual mean-field argument, is expected to result in nematic ordering.

We check and extend this argument by solving the phase-field model numerically for 360 cells (see Supplemental Material for details [38]). For strong cell-cell adhesion $\omega = 0.5$, the cells are extended and aligned and become jammed in the configuration shown in Fig. 1(e). Decreasing the cell-cell adhesion to zero weakens the alignment and allows the cells to move collectively. We observe the well-known splay instability that characterizes contractile active nematics, and which leads to active turbulence. Topological defects are continually created and destroyed. These move toward their tail confirming that they result from contractile forces [Figs. 2(a)–2(d) and Supplemental Material, Video 1 [38] ].

*Intercellular extensile forces.*—Although a contractile, intercellular force is more physical, it is interesting to compare extensile forcing ($\zeta_{\text{inter}} > 0$). In this case, the alignment due to effective self-interactions is frustrated and there is no long-range ordering. Instead, cells tend to align locally, at the scale of a few cells, in a capped line structure [Figs. 1(f), 2(e), and Supplemental Material, Video 2 [38] ]. Measuring the average velocity field around defects confirms that they move tail to head as expected in an extensile system [Figs. 2(e)–2(h)]. Defects form more easily, and are more localized and less persistent than in the contractile case [note the different scales of Figs. 2(d) and 2(h)].

It is of interest that similar capped line structures are seen in simulations of hard rods driven by a polar force [45,46].

*Fluctuations.*—We next model the strong fluctuations in cell shape that are observed in many epithelial cell layers by including the anisotropic noise term defined in Eq. (5), in the equation governing the relaxation of a cell director Eq. (4). This leads to anisotropic fluctuations of the intercellular forces. If the relaxation of the director to the long axis of a cell is rapid compared to the timescale of cell reorientation, Eq. (4) can be integrated to give

$$\mathbf{n}^{(i)} = \mathbf{n}^{(i)}_0 e^{-J_n t} + \mathbf{d}^{(i)}_{\parallel}(1 - e^{-J_n t}) + \int_0^t ds\, \boldsymbol{\eta}(s) e^{-J_n(t-s)}, \tag{10}$$

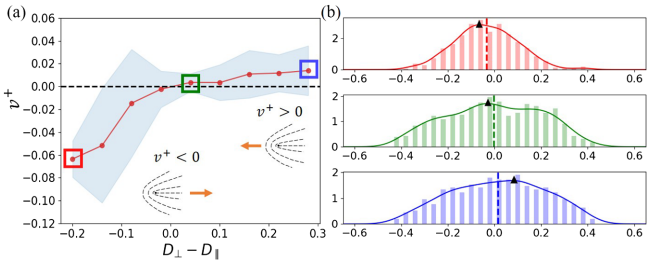


FIG. 3. (a) Velocity of the $+1/2$ defects along their tail to head direction $v^+$ as the magnitude of the fluctuations along the short axis of the cells $D_\perp$ is varied. The red line is the average velocity, and the light blue background denotes the standard error. (b) Histogram of $v^+$ for 201 (red), 401 (green), 305 (blue) defects corresponding to framed points in (a). Vertical dashed lines: mean value. Black triangles: maximum of the smoothed histogram. $\zeta_{\text{inter}} = -0.6$, $D_\parallel = 0.2$, $\omega = 0.0$.

where $\mathbf{n}^{(i)}_0$ is the director of cell $i$ at $t = 0$. Note that $\langle \mathbf{n}^{(i)} \rangle \approx \mathbf{d}^{(i)}_{\parallel}$ for times longer than the relaxation timescale. Thus, $\mathbf{n}^{(i)}$ is not of unit length (this is only true for its mean value) but fluctuates around $d^{(i)}_{\parallel}$, the unit vector along the elongation axis. Using this expression in Eqs. (7) and (8) the averaged intercellular force follows as

$$\langle \mathbf{f}^{(i)}_{\text{active}}(\mathbf{x}) \rangle \approx -\zeta_{\text{inter}} \left(1 + \frac{D_\parallel - D_\perp}{2J_n}\right) \times \sum_{j\neq i} \left(\mathbf{d}^{(j)}_{\parallel}\mathbf{d}^{(j)T}_{\parallel} - \frac{1}{2}\mathbb{1}\right) \cdot \nabla\varphi^{(j)}(\mathbf{x}). \tag{11}$$

Hence, fluctuations in cell shape along $\mathbf{d}_\perp$ tend to change the sign of the activity.

This is confirmed in Fig. 3 where we plot the defect velocity against $D_\perp - D_\parallel$, showing a change from contractile to extensile behavior (see also Fig. S3 and Videos 3 and 4 in the Supplemental Material [38]). Further evidence for a crossover is presented in Supplemental Material, Fig. S4 [38] where the distribution of the angles between the long axes of neighboring cells is plotted. With increasing $D_\perp$ there is a crossover from a peak at 0° signaling nematic ordering to two weaker peaks at 0° and 90° indicating the capped line state. Note that anisotropic fluctuations can also allow the reverse process, a change from extensile behavior to contractile behavior. When extensile and contractile influences balance (green square in Fig. 3), a jammed phase emerges where the shape of cells is round on average, but fluctuates strongly (Supplemental Material, Video 5 [38]).

Our work gives an explanation for why cells that are, on average, circular can exhibit nematic ordering and active turbulence in terms of fundamental, active, interactions between the cells. It also shows that the direction of motion of active defects can vary. We argue that intercellular forces mediated through cell-cell junctions can lead to contractile

behavior. Anisotropic fluctuations in these forces (perpendicular to the long axis of the cell) can then drive the system extensile. By contrast, work in Refs. [31–33] has shown that fluctuating polar forces can result in extensile or contractile stresses.

Our prediction that the activity of confluent cell layers depends on anisotropic fluctuations of intercellular forces and hence on cell shape could be tested experimentally by analyzing the dynamical evolution of monolayers.

We thank Amin Doostmohammadi for helpful discussions on the model and Mehrana Raesian Nejad, James Graham, and Liam Ruske for their critical reading of the manuscript. G. Z. acknowledges support from the China Scholarship Council (Grant No. 201808220082), the University of Oxford and the Rudolf Peierls Centre for Theoretical Physics.

*Corresponding author.
guanming.zhang@physics.ox.ac.uk

[1] X. Trepat, M. R. Wasserman, T. E. Angelini, E. Millet, D. A. Weitz, J. P. Butler, and J. J. Fredberg, Nat. Phys. **5**, 426 (2009).
[2] B. Ladoux and R.-M. Mège, Nat. Rev. Mol. Cell Biol. **18**, 743 (2017).
[3] D. Boocock, N. Hino, N. Ruzickova, T. Hirashima, and E. Hannezo, Nat. Phys. **17**, 267 (2021).
[4] R. Mueller, J. M. Yeomans, and A. Doostmohammadi, Phys. Rev. Lett. **122**, 048004 (2019).
[5] G. Peyret, R. Mueller, J. d'Alessandro, S. Begnaud, P. Marcq, R.-M. Mège, J. M. Yeomans, A. Doostmohammadi, and B. Ladoux, Biophys. J. **117**, 464 (2019).
[6] G. Zhang, R. Mueller, A. Doostmohammadi, and J. M. Yeomans, J. R. Soc. Interface **17**, 20200312 (2020).
[7] J. Löber, F. Ziebert, and I. S. Aranson, Soft Matter **10**, 1365 (2014).
[8] J. Löber, F. Ziebert, and I. S. Aranson, Sci. Rep. **5**, 9172 (2015).
[9] D. Wenzel, S. Praetorius, and A. Voigt, J. Chem. Phys. **150**, 164108 (2019).
[10] B. Loewe, M. Chiang, D. Marenduzzo, and M. C. Marchetti, Phys. Rev. Lett. **125**, 038003 (2020).
[11] B. Palmieri, Y. Bresler, D. Wirtz, and M. Grant, Sci. Rep. **5**, 11745 (2015).
[12] R. Farhadifar, J.-C. Röper, B. Aigouy, S. Eaton, and F. Jülicher, Curr. Biol. **17**, 2095 (2007).
[13] D. Bi, J. Lopez, J. M. Schwarz, and M. L. Manning, Nat. Phys. **11**, 1074 (2015).
[14] F. Giavazzi, M. Paoluzzi, M. Macchi, D. Bi, G. Scita, M. L. Manning, R. Cerbino, and M. C. Marchetti, Soft Matter **14**, 3471 (2018).
[15] D. Bi, X. Yang, M. C. Marchetti, and M. L. Manning, Phys. Rev. X **6**, 021011 (2016).
[16] S. Alt, P. Ganguly, and G. Salbreux, Phil. Trans. R. Soc. B **372**, 20150520 (2017).
[17] B. Alberts, A. Johnson, J. Lewis, M. Raff, K. Roberts, P. Walter, D. Bray, and J. D. Watson, *Molecular Biology of the Cell* (W. W. Norton & Company, New York, 2003), Vol. 32.
[18] T. Mitchison and L. Cramer, Cell **84**, 371 (1996).
[19] B. R. Sarangi, M. Gupta, B. L. Doss, N. Tissot, F. Lam, R.-M. Mège, N. Borghi, and B. Ladoux, Nano Lett. **17**, 399 (2017).
[20] J. T. Parsons, A. R. Horwitz, and M. A. Schwartz, Nat. Rev. Mol. Cell Biol. **11**, 633 (2010).
[21] T. D. Pollard and G. G. Borisy, Cell **112**, 453 (2003).
[22] M. Sadati, N. T. Qazvini, R. Krishnan, C. Y. Park, and J. J. Fredberg, Differentiation (Berlin) **86**, 121 (2013).
[23] C. Blanch-Mercader, V. Yashunsky, S. Garcia, G. Duclos, L. Giomi, and P. Silberzan, Phys. Rev. Lett. **120**, 208101 (2018).
[24] L. Balasubramaniam, A. Doostmohammadi, T. B. Saw, G. H. N. S. Narayana, R. Mueller, T. Dang, M. Thomas, S. Gupta, S. Sonam, A. S. Yap *et al.*, Nat. Mater. **20**, 1 (2021).
[25] T. B. Saw, A. Doostmohammadi, V. Nier, L. Kocgozlu, S. Thampi, Y. Toyama, P. Marcq, C. T. Lim, J. M. Yeomans, and B. Ladoux, Nature (London) **544**, 212 (2017).
[26] K. Kawaguchi, R. Kageyama, and M. Sano, Nature (London) **545**, 327 (2017).
[27] T. Sanchez, D. T. Chen, S. J. DeCamp, M. Heymann, and Z. Dogic, Nature (London) **491**, 431 (2012).
[28] C. Dombrowski, L. Cisneros, S. Chatkaew, R. E. Goldstein, and J. O. Kessler, Phys. Rev. Lett. **93**, 098103 (2004).
[29] A. Doostmohammadi, J. Ignés-Mullol, J. M. Yeomans, and F. Sagués, Nat. Commun. **9**, 3246 (2018).
[30] L. Giomi, M. J. Bowick, P. Mishra, R. Sknepnek, and M. C. Marchetti, Phil. Trans. R. Soc. A **372**, 20130365 (2014).
[31] F. Vafa, M. J. Bowick, B. I. Shraiman, and M. C. Marchetti, Soft Matter **17**, 3068 (2021).
[32] A. Patelli, I. Djafer-Cherif, I. S. Aranson, E. Bertin, and H. Chaté, Phys. Rev. Lett. **123**, 258001 (2019).
[33] A. Killeen, T. Bertrand, and C. F. Lee, Phys. Rev. Lett. **128**, 078001 (2022).
[34] M. Abercrombie, In vitro **6**, 128 (1970).
[35] B. Stramer and R. Mayor, Nat. Rev. Mol. Cell Biol. **18**, 43 (2017).
[36] F. Ziebert, S. Swaminathan, and I. S. Aranson, J. R. Soc. Interface **9**, 1084 (2012).
[37] F. Ziebert and I. S. Aranson, PLoS One **8**, e64511 (2013).
[38] See Supplemental Material at http://link.aps.org/supplemental/10.1103/PhysRevLett.130.038202 for more details of the phase-field model and the simulation approaches and additional figures showing defect properties, which includes Ref. [39].
[39] A. J. Vromans and L. Giomi, Soft Matter **12**, 6490 (2016).
[40] M. E. Cates and E. Tjhung, J. Fluid Mech. **836**, P1 (2018).
[41] J. Bigun and G. H. Granlund, in *Proceedings of the 1st International Conference on Computer Vision* (IEEE Computer Society Press, London, 1987), pp. 433–438.
[42] R. A. Simha and S. Ramaswamy, Phys. Rev. Lett. **89**, 058101 (2002).
[43] A. Bretscher, K. Edwards, and R. G. Fehon, Nat. Rev. Mol. Cell Biol. **3**, 586 (2002).
[44] Y. Senju and F.-C. Tsai, Biophys. Rev. Lett. **14**, 199 (2022).
[45] O. J. Meacock, A. Doostmohammadi, K. R. Foster, J. M. Yeomans, and W. M. Durham, Nat. Phys. **17**, 205 (2021).
[46] H. H. Wensink, J. Dunkel, S. Heidenreich, K. Drescher, R. E. Goldstein, H. Löwen, and J. M. Yeomans, Proc. Natl. Acad. Sci. U.S.A. **109**, 14308 (2012).